REPORT 1042

SOME EFFECTS OF NONLINEAR VARIATION IN THE DIRECTIONAL-STABILITY AND DAMPING-IN-YAWING DERIVATIVES ON THE LATERAL STABILITY OF AN AIRPLANE[1]

By Leonard Sternfield

SUMMARY

A theoretical investigation has been made to determine the effect of nonlinear stability derivatives on the lateral stability of an airplane. Motions were calculated on the assumption that the directional-stability and the damping-in-yawing derivatives are functions of the angle of sideslip. The application of the Laplace transform to the calculation of an airplane motion when certain types of nonlinear derivatives are present is described in detail. The types of nonlinearities assumed correspond to the condition in which the values of the directional-stability and damping-in-yawing derivatives are zero for small angles of sideslip.

The results of the investigation indicated that under certain conditions the nonlinear stability derivatives assumed in the analysis caused a motion which had different rates of damping for the large and small amplitudes of motion, with very little damping at the small amplitudes. In general, the period of the resultant oscillation increased with time.

INTRODUCTION

Recent flight tests of several airplanes designed for high-speed high-altitude flight have indicated neutrally damped lateral oscillations of small amplitude generally referred to as snaking. Upon examination of the flight records, the decrement of the oscillatory motion is found in some cases to be different for the large and small amplitudes of motion with a neutrally stable oscillation occurring at the small amplitudes. One of the explanations offered for the cause of this type of motion is that some of the stability derivatives are nonlinear; that is, the derivatives have different values for the large and small amplitudes of motion. The nonlinearity could be caused by boundary-layer effects or flow separation due to poor fairing at the junction of the tail surfaces.

The present report represents a preliminary investigation of the effect of the presence of two nonlinear stability derivatives, the directional-stability derivative C_{n_β} and the damping-in-yawing derivative C_{n_r}, on the motion of an airplane. These derivatives were selected for the analysis since the damping of the oscillation is a function of C_{n_r} and since C_{n_r} depends upon the C_{n_β} contributed by the tail. The derivatives C_{n_β} and C_{n_r} were both assumed to be functions of the sideslip angle β. Calculations were made of the airplane motion due to a disturbance in sideslip for three different types of nonlinearities.

SYMBOLS AND COEFFICIENTS

ϕ	angle of roll, radians
ψ	angle of yaw, radians
β	angle of sideslip, radians except where noted in figures (v/V)
r	yawing angular velocity, radians per second $(d\psi/dt)$
p	rolling angular velocity, radians per second $(d\phi/dt)$
v	sideslip velocity along the Y-axis, feet per second
V	airspeed, feet per second
ρ	mass density of air, slugs per cubic foot
q	dynamic pressure, pounds per square foot $\left(\frac{1}{2}\rho V^2\right)$
b	wing span, feet
S	wing area, square feet
W	weight of airplane, pounds
m	mass of airplane, slugs (W/g)
g	acceleration due to gravity, feet per second per second
μ_b	relative density factor $(m/\rho Sb)$
η	inclination of principal longitudinal axis of airplane with respect to flight path, positive when principal axis is above flight path at the nose, degrees
γ	angle of flight path to horizontal axis, positive in climb, degrees
k_{X_0}	radius of gyration in roll about principal longitudinal axis, feet
k_{Z_0}	radius of gyration in yaw about principal vertical axis, feet
K_{X_0}	nondimensional radius of gyration in roll about principal longitudinal axis (k_{X_0}/b)

[1] Supersedes NACA TN 2233, "Some Effects of Nonlinear Variation in the Directional-Stability and Damping-in-Yawing Derivatives on the Lateral Stability of an Airplane" by Leonard Sternfield, 1950.

K_{Z_0} nondimensional radius of gyration in yaw about principal vertical axis (k_{Z_0}/b)

K_X nondimensional radius of gyration in roll about longitudinal stability axis ($\sqrt{K_{X_0}^2 \cos^2 \eta + K_{Z_0}^2 \sin^2 \eta}$)

K_Z nondimensional radius of gyration in yaw about vertical stability axis ($\sqrt{K_{Z_0}^2 \cos^2 \eta + K_{X_0}^2 \sin^2 \eta}$)

K_{XZ} nondimensional product-of-inertia parameter ($(K_{Z_0}^2 - K_{X_0}^2) \sin \eta \cos \eta$)

C_L trim lift coefficient $\left(\frac{W \cos \gamma}{qS}\right)$

C_l rolling-moment coefficient $\left(\frac{\text{Rolling moment}}{qSb}\right)$

C_n yawing-moment coefficient $\left(\frac{\text{Yawing moment}}{qSb}\right)$

C_Y lateral-force coefficient $\left(\frac{\text{Lateral force}}{qS}\right)$

$C_{l_\beta} = \frac{\partial C_l}{\partial \beta}$

$C_{n_\beta} = \frac{\partial C_n}{\partial \beta}$

$C_{Y_\beta} = \frac{\partial C_Y}{\partial \beta}$

$C_{n_r} = \frac{\partial C_n}{\partial \left(\frac{rb}{2V}\right)}$

$C_{n_p} = \frac{\partial C_n}{\partial \left(\frac{pb}{2V}\right)}$

$C_{l_p} = \frac{\partial C_l}{\partial \left(\frac{pb}{2V}\right)}$

$C_{Y_p} = \frac{\partial C_Y}{\partial \left(\frac{pb}{2V}\right)}$

$C_{Y_r} = \frac{\partial C_Y}{\partial \left(\frac{rb}{2V}\right)}$

$C_{l_r} = \frac{\partial C_l}{\partial \left(\frac{rb}{2V}\right)}$

C_{n_c} yawing-moment constant

t time, seconds

s_b nondimensional time parameter based on span (Vt/b)

D_b differential operator $\left(\frac{d}{ds_b}\right)$

σ operator in Laplace transformation

$T_{1/2}$ time for amplitude of oscillation to damp to one-half its original value, seconds

The subscript 0 is used to indicate initial conditions and a bar is used to denote variables in the operational equations.

ANALYSIS

NONLINEAR STABILITY DERIVATIVES

The assumptions made with regard to the nonlinearity of the stability derivatives C_{n_β} and C_{n_r} are shown in figure 1.

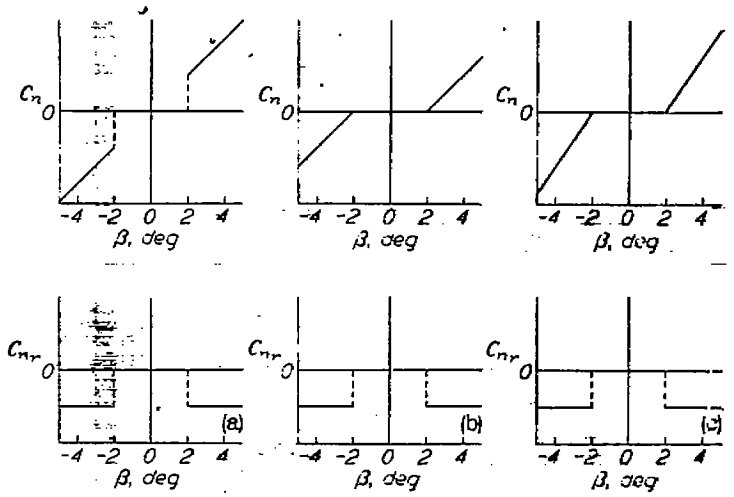

(a) Case 1. (b) Case 2. (c) Case 3.

FIGURE 1.—Three types of nonlinear stability derivatives assumed in the analysis.

For all three cases presented in the figure, C_n is equal to zero for $-2° < \beta < 2°$, a region which is subsequently referred to as a dead spot. Thus when the airplane is within the dead spot, the value of the directional stability derivative C_{n_β} is zero. Since the damping-in-yawing derivative C_{n_r} is a direct function of C_{n_β} contributed by the tail, C_{n_r} was also assumed to be zero for values of $-2° < \beta < 2°$. In the region outside of the dead spot, each one of the cases represents a different type of variation of C_n with β in order to simulate the effect of several possible flow conditions on the side force acting on the vertical surface. For cases 1 and 2, $C_{n_\beta} = 0.28$ and for case 3, $C_{n_\beta} = 0.41$. The corresponding value of C_{n_r} for all three cases is -0.39. It should be noted in figure 1 that for cases 2 and 3, $C_n = 0$ at β of 2° and $-2°$, whereas for case 1, C_n has a finite value at β of 2° and $-2°$.

METHOD OF CALCULATING MOTION

Since the nonlinearities shown in figure 1 can be treated as linear derivatives of different values within and outside of the dead spot, the airplane motion is calculated on the basis of classical linear theory. The equations of motion and the general method of calculating the motion of an airplane are given in references 1 and 2. The methods of references 1 and 2 are based on the Laplace transformation which inherently takes into account the initial conditions of the problem. Because the Laplace transformation considers the initial displacements and initial velocities of the problem, this method is directly applicable to the calculation of the motion of an airplane which has nonlinear derivatives similar to the derivatives presented in figure 1.

The nondimensional linearized lateral equations of motion, referred to the stability axes, are for rolling, for yawing, and for sideslipping, respectively:

$$\left.\begin{aligned}
2\mu_b(K_X^2 D_b^2\phi + K_{XZ} D_b^2\psi) &= C_{l_\beta}\beta + \frac{1}{2}C_{l_p} D_b\phi + \frac{1}{2}C_{l_r} D_b\psi \\
2\mu_b(K_Z^2 D_b^2\psi + K_{XZ} D_b^2\phi) &= C_{n_\beta}\beta + \frac{1}{2}C_{n_p} D_b\phi + \frac{1}{2}C_{n_r} D_b\psi + C_{n_c} \\
2\mu_b(D_b\beta + D_b\psi) &= C_{Y_\beta}\beta + \frac{1}{2}C_{Y_p} D_b\phi + C_L\phi + \frac{1}{2}C_{Y_r} D_b\psi + \\
&\quad (C_L \tan \gamma)\psi
\end{aligned}\right\} \tag{1}$$

The Laplace transformation of equations (1), with the use of the symbol σ for the operator, is

$$\left.\begin{aligned}
&\left(2\mu_b K_X^2\sigma^2-\frac{1}{2}C_{l_p}\sigma\right)\bar{\phi}+\left(2\mu_b K_{XZ}\sigma^2-\frac{1}{2}C_{l_r}\sigma\right)\bar{\psi}-C_{l_\beta}\bar{\beta}=2\mu_b K_X^2[\sigma\phi_0+(D_b\phi)_0]-\frac{1}{2}C_{l_p}\phi_0+2\mu_b K_{XZ}[\sigma\psi_0+(D_b\psi)_0]-\frac{1}{2}C_{l_r}\psi_0\\
&\left(2\mu_b K_{XZ}\sigma^2-\frac{1}{2}C_{n_p}\sigma\right)\bar{\phi}+\left(2\mu_b K_Z^2\sigma^2-\frac{1}{2}C_{n_r}\sigma\right)\bar{\psi}-C_{n_\beta}\bar{\beta}=2\mu_b K_{XZ}[\sigma\phi_0+(D_b\phi)_0]-\frac{1}{2}C_{n_p}\phi_0+2\mu_b K_Z^2[\sigma\psi_0+(D_b\psi)_0]-\frac{1}{2}C_{n_r}\psi_0+\frac{C_{n_c}}{\sigma}\\
&\left(-\frac{1}{2}C_{Y_p}\sigma-C_L\right)\bar{\phi}+\left(2\mu_b\sigma-\frac{1}{2}C_{Y_r}\sigma-C_L\tan\gamma\right)\bar{\psi}+(2\mu_b\sigma-C_{Y_\beta})\bar{\beta}=-\frac{1}{2}C_{Y_p}\phi_0+\left(2\mu_b-\frac{1}{2}C_{Y_r}\right)\psi_0+2\mu_b\beta_0
\end{aligned}\right\}\quad(2)$$

Equations (2) represent three simultaneous algebraic equations which can be solved for $\bar{\beta}$, $\bar{\phi}$, $\bar{\psi}$, and their derivatives by the method of determinants. For example,

$$\bar{\beta}=\frac{\bar{\Delta}_1}{\bar{\Delta}}=\frac{f(\sigma)}{F(\sigma)}\quad(3)$$

where $\bar{\Delta}$ is the characteristic lateral-stability equation

$$(A\sigma^4+B\sigma^3+C\sigma^2+D\sigma+E)\sigma$$

and

$$\bar{\Delta}_1=A_1\sigma^4+B_1\sigma^3+C_1\sigma^2+D_1\sigma+E_1$$

The expressions for A, B, C, D, and E, in terms of the mass and aerodynamic parameters of the airplane, are given on pages 27 and 28 of reference 1. The coefficients of the $\bar{\Delta}_1$ equation are

$$A_1=\beta_0[8\mu_b^3(K_X^2K_Z^2-K_{XZ}^2)]$$

$$\begin{aligned}
B_1=&\phi_0[4\mu_b^2C_L(K_X^2K_Z^2-K_{XZ}^2)]+(D_b\phi)_0[2\mu_b^2C_{Y_p}(K_X^2K_Z^2-K_{XZ}^2)]+\psi_0[4\mu_b^2C_L\tan\gamma(K_X^2K_Z^2-K_{XZ}^2)]+\\
&(D_b\psi)_0[2\mu_b^2(C_{Y_r}-4\mu_b)(K_X^2K_Z^2-K_{XZ}^2)]+\beta_0[2\mu_b^2(K_{XZ}C_{l_r}-K_X^2C_{n_r})+2\mu_b^2(K_{XZ}C_{n_p}-K_Z^2C_{l_p})]
\end{aligned}$$

$$\begin{aligned}
C_1=&\phi_0[\mu_bC_L(K_{XZ}C_{l_r}-K_X^2C_{n_r})+\mu_bC_L(K_{XZ}C_{n_p}-K_Z^2C_{l_p})]+(D_b\phi)_0\left[\frac{1}{2}\mu_bK_X^2(C_{n_p}C_{Y_r}-C_{n_r}C_{Y_p})+\right.\\
&\left.2\mu_b^2K_X^2(2K_Z^2C_L-C_{n_p})+2\mu_b^2K_{XZ}(C_{l_p}-2K_{XZ}C_L)+\frac{1}{2}\mu_bK_{XZ}(C_{l_r}C_{Y_p}-C_{l_p}C_{Y_r})\right]+\psi_0[\mu_bC_L\tan\gamma(K_{XZ}C_{l_r}-C_{n_r}K_X^2)+\\
&\mu_bC_L\tan\gamma(K_{XZ}C_{n_p}-K_Z^2C_{l_p})]+(D_b\psi)_0\left[\frac{1}{2}\mu_bK_{XZ}(C_{n_p}C_{Y_r}-C_{n_r}C_{Y_p})+\frac{1}{2}\mu_bK_Z^2(C_{l_r}C_{Y_p}-C_{l_p}C_{Y_r})+\right.\\
&\left.4\mu_b^2C_L\tan\gamma(K_X^2K_Z^2-K_{XZ}^2)+2\mu_b^2(K_Z^2C_{l_p}-K_{XZ}C_{n_p})\right]+\beta_0\left[\frac{1}{2}\mu_b(C_{l_p}C_{n_r}-C_{l_r}C_{n_p})\right]+\\
&C_{n_c}[-\mu_bK_{XZ}C_{Y_p}+\mu_bK_X^2C_{Y_r}-4\mu_b^2K_X^2]
\end{aligned}$$

$$\begin{aligned}
D_1=&\phi_0\left[\frac{1}{4}C_L(C_{l_p}C_{n_r}-C_{l_r}C_{n_p})\right]+(D_b\phi)_0[\mu_bC_L\tan\gamma(K_X^2C_{n_p}-K_{XZ}C_{l_p})+\mu_bC_L(K_{XZ}C_{l_r}-K_X^2C_{n_r})]+\\
&\psi_0\left[\frac{1}{4}C_L\tan\gamma(C_{l_p}C_{n_r}-C_{l_r}C_{n_p})\right]+(D_b\psi)_0[\mu_bC_L(K_Z^2C_{l_r}-K_{XZ}C_{n_r})+\mu_bC_L\tan\gamma(K_{XZ}C_{n_p}-K_Z^2C_{l_p})]+\\
&C_{n_c}\left[\frac{1}{4}C_{Y_p}C_{l_r}-2\mu_bK_{XZ}C_L+2\mu_bK_X^2C_L\tan\gamma+\mu_bC_{l_p}-\frac{1}{4}C_{l_p}C_{Y_r}\right]
\end{aligned}$$

$$E_1=C_{n_c}\left(\frac{1}{2}C_LC_{l_r}-\frac{1}{2}C_{l_p}C_L\tan\gamma\right)$$

The solution of equation (3), which will result in a time history of β as a function of s_b, is obtained from the Heaviside expansion theorem (reference 3):

$$\beta=\sum_{n=1}^{m}\frac{f(\lambda_n)}{F'(\lambda_n)}e^{\lambda_n s_b}\quad(4)$$

where λ_n are the roots of $F(\sigma)$ set equal to zero. Similar solutions are derived for ϕ, ψ, $D_b\phi$, $D_b\psi$, and $D_b\beta$. The time scale is readily converted from s_b units to t units by the equation $t=\frac{b}{V}s_b$.

The values of the stability derivatives and mass characteristics used in the calculations are presented in table I. The table is divided into two columns which differ only in the values of C_{n_β} and C_{n_r} of the airplane for the cases where the

TABLE I

STABILITY DERIVATIVES AND MASS CHARACTERISTICS OF THE AIRPLANE CONSIDERED IN THE ANALYSIS

Derivative or characteristic	Outside of dead spot	Within dead spot
W/S, lb/ft^2	80	80
μ_b	101.1	101.1
ρ, slugs/ft^3	0.00089	0.00089
V, ft/sec	753	753
C_L	0.318	0.318
b, ft	27.7	27.7
γ, deg	0	0
K_Z^2	0.0573	0.0573
K_X^2	0.0069	0.0069
C_{l_p}, per radian	−0.462	−0.462
C_{n_p}, per radian	−0.0155	−0.0155
C_{l_β}, per radian	−0.126	−0.126
C_{Y_p}, per radian	0	0
C_{Y_r}, per radian	0	0
η, deg	−2.0, 0, 2.0	−2.0, 0, 2.0
C_{n_r}, per radian	−0.392	0
C_{n_β} (cases 1 and 2), per radian	0.28	0
C_{n_β} (case 3), per radian	0.41	0

airplane is either outside of or within the dead spot. From the analytical solution of the motion, based on the mass and aerodynamic characteristics of the first column of table I and an initial condition of $\beta=5°$, the time history of β was computed for several values of s_b until the value of s_b for which $\beta=2°$ was reached. For values of s_b greater than the s_b which results in $\beta=2°$, this analytical solution is incorrect since the airplane has now entered into the dead spot and the values of C_{n_β} and C_{n_r} are zero. Thus, a new solution must be calculated with the use of the values given in the second column of table I with new initial conditions. The new initial conditions are determined by substituting the value of s_b at which $\beta=2°$ in the original analytical solutions of ϕ, ψ, $D_b\phi$, $D_b\psi$, and $D_b\beta$. Once these initial conditions are known, another set of analytical solutions are computed for β, ϕ, ψ, and their derivatives from equations (3) and (4). This procedure is followed every time β crosses through 2° or −2°. The final resultant motion in sideslip is the sum of all the analytical solutions in β, each one of which is correct only for a particular interval of time.

The constant C_{n_c} is introduced into the yawing-moment equation of equations (1), since the value of the yawing-moment coefficient due to sideslip is $C_{n_\beta}\beta+C_{n_c}$ for the condition of the airplane having the dead spot in cases 2 and 3 of figure 1. The values of C_{n_c} are $|0.00977|$ and $|0.0143|$ for cases 2 and 3, respectively. The sign of C_{n_c} is opposite to that of β. For case 1 of figure 1, $C_{n_c}=0$.

It is apparent that the procedure employed is a time-consuming process and subject to the possibility of many computational errors due to the magnitude of the computations. The final solution can be obtained, however, in a relatively short time through the use of automatic digital computing machines.

RESULTS AND DISCUSSION

The effect of the nonlinear stability derivatives on the lateral motion was investigated for the airplane described by the mass and aerodynamic characteristics given in table I, with three different values for the damping of the lateral oscillation as calculated on the basis of derivatives constant with amplitude. Since the damping was varied arbitrarily by assuming different values for the angle of inclination of the principal longitudinal axis of the airplane to the flight path η, three values of η, −2°, 0°, and 2°, were selected which correspond to a damping of the lateral oscillation, expressed in terms of $T_{1/2}$, of 5.6, 3.0, and 1.8, respectively. The motion of the airplane in sideslip, due to an initial disturbance in sideslip of 5°, for the three values of η is shown in figure 2. Since these motions are calculated on the assumption of derivatives constant with amplitude, the amplitudes of the motion decrease exponentially with time and will eventually reduce to zero. As can be noted in the first column of table I, the C_{n_β} for cases 1 and 2 is 0.28; whereas the C_{n_β} for case 3 is 0.41. The motions presented in figure 2 are for $C_{n_\beta}=0.28$; however, the motions for $C_{n_\beta}=0.41$ would exhibit oscillations of approximately the same damping and a slightly smaller period.

The motions of the airplane in sideslip, showing the effect of the nonlinearities illustrated in figures 1(a), 1(b), and 1(c), are presented in figures 3 to 5, respectively. In all cases, an initial disturbance in sideslip of 5° was assumed. The pronounced effect of the nonlinearities on the lateral motion is noted by a comparison of figure 2 and either one of figures 3, 4, or 5. In all three figures (figs. 3 to 5) the motion for $\eta=2°$, the most stable case, approaches a constant value. The analytical solution of the motion for the case of $\eta=2°$ in figure 3 indicates that, within the dead spot, the airplane will oscillate at a period of 6.56 seconds and $T_{1/2}=3.38$ seconds and will eventually approach the value of $\beta=-0.0092°$. Similar motions would be obtained for the case of $\eta=2°$ in figures 4 and 5. As η is decreased, the damping of the oscillatory motion depends upon the nonlinearity assumed and the values of η. In figure 3, the motion for $\eta=0°$ damps at a slow rate at the large amplitudes until the oscillation reaches an amplitude of approximately 2.4° where the damping of the oscillation is zero. The period of the oscillation increases from 1.5 to 1.85 seconds. For the case of $\eta=-2°$, a very lightly damped oscillation is apparent within the first few seconds and the airplane may be considered to be neutrally stable at an amplitude of ∓4.5°. In figures 4 and 5 the motion for $\eta=0°$ clearly indicates that the damping is decreasing as the amplitude decreases and the period of the oscillation increases; for $\eta=-2°$, the oscillatory motion is slightly unstable. A neutrally stable oscillation would be expected to occur in figures 4 and 5 for the combinations of a value of η between 0° and −2° and the dead spot assumed in the calculations or for $\eta=-2°$ and a smaller dead spot.

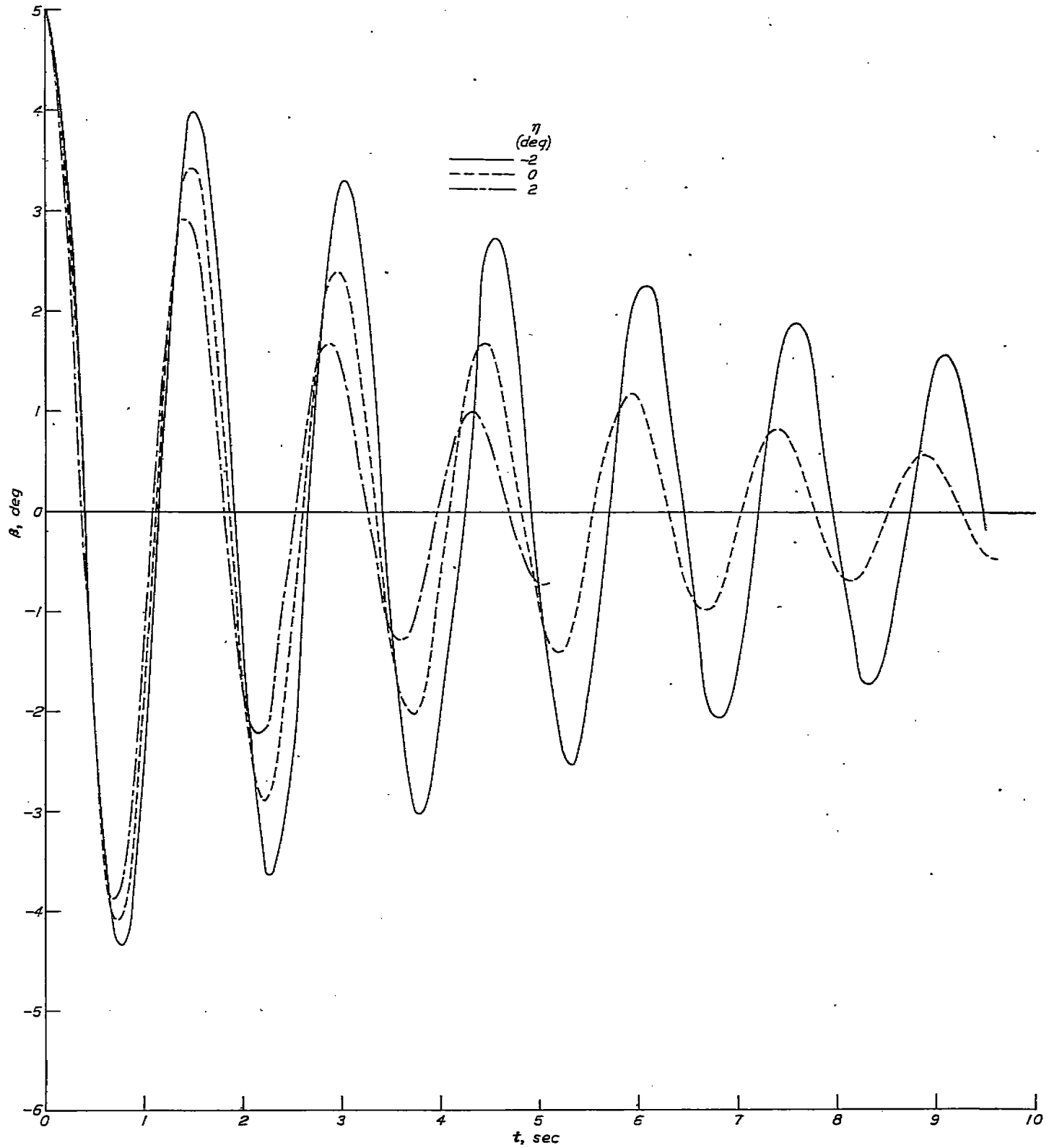

FIGURE 2.—Calculated motion of an airplane due to an initial disturbance in sideslip for several values of η.

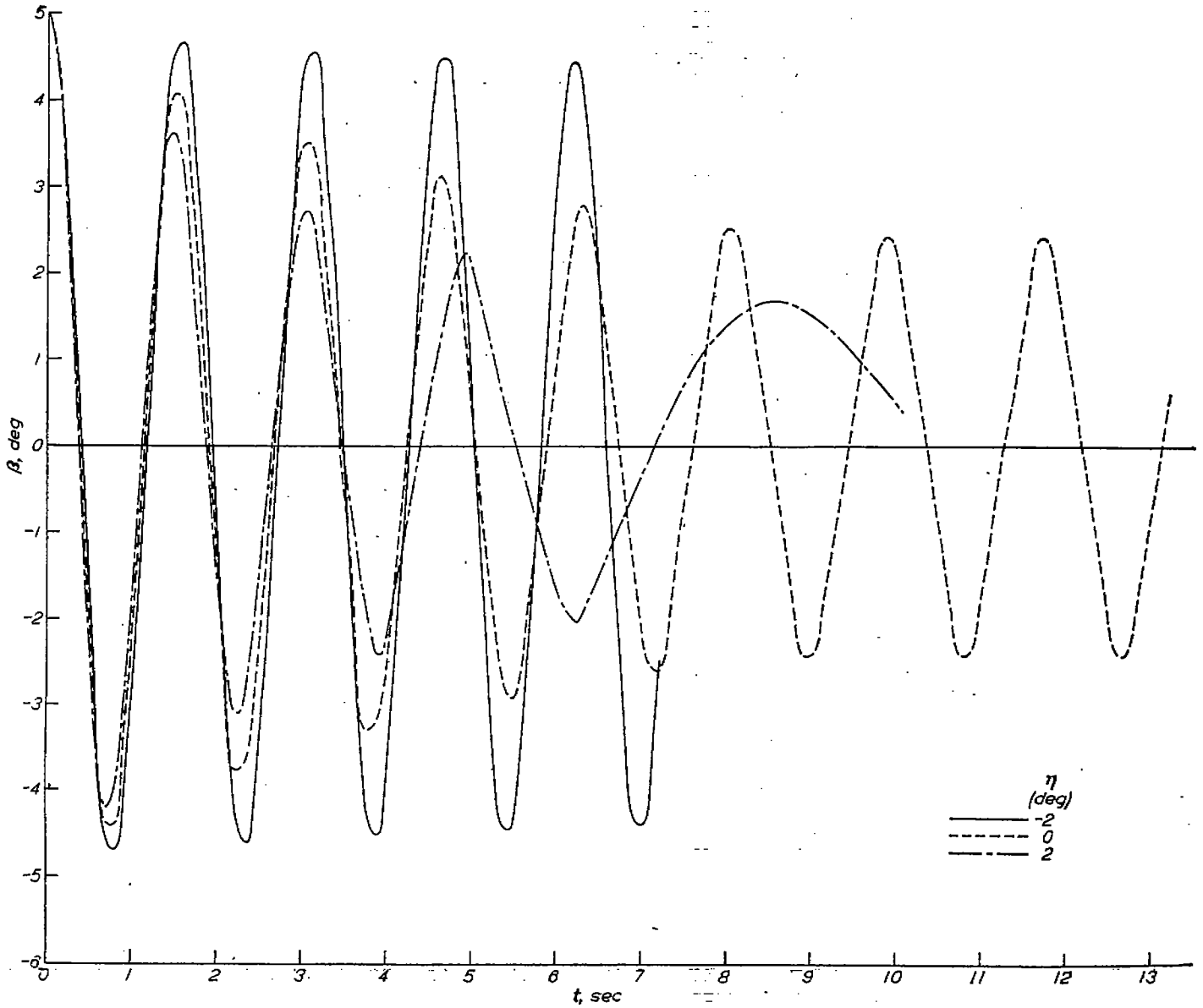

FIGURE 3.—The effect of the nonlinear derivatives described in figure 1(a) on the motion of an airplane.

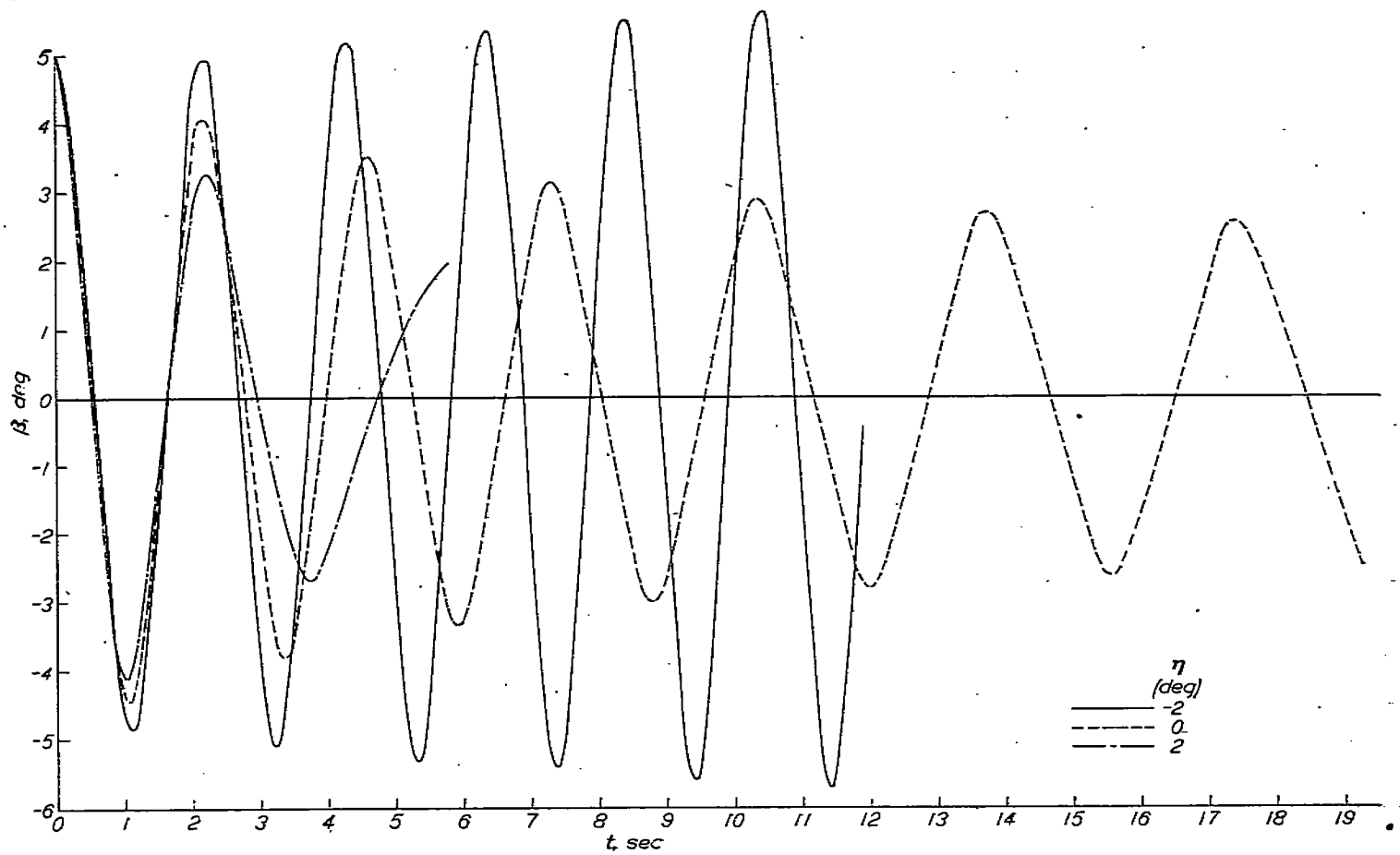

FIGURE 4.—The effect of the nonlinear derivatives described in figure 1(b) on the motion of an airplane.

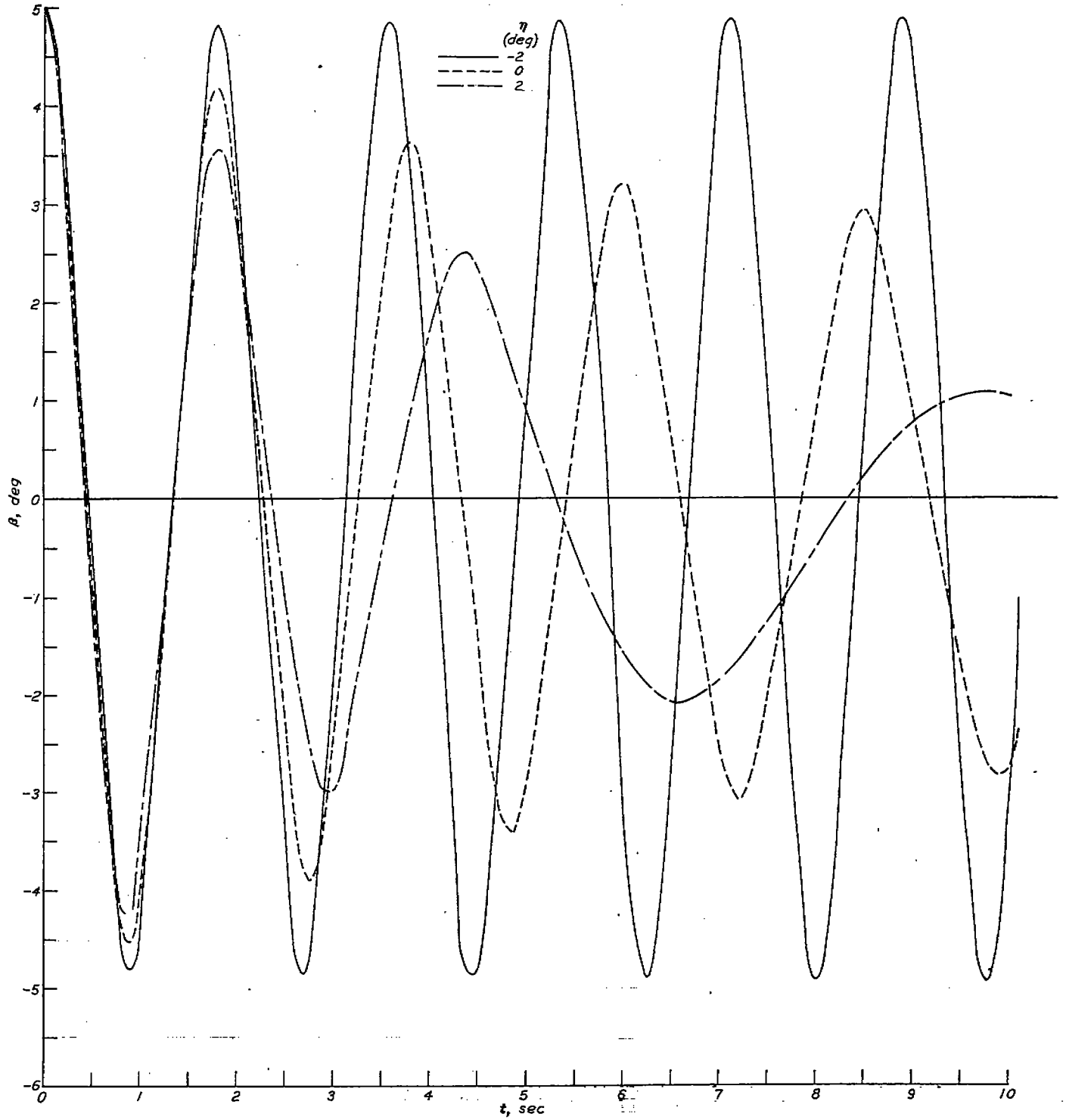

FIGURE 5.—The effect of the nonlinear derivatives described in figure 1(c) on the motion of an airplane.

In general, the results indicate that the damping of the lateral oscillation calculated with the use of derivatives constant with amplitude is a determining factor in the type of motion obtained where nonlinear derivatives are present. As the inherent damping of the lateral oscillation decreases, a smaller dead spot will result in a neutrally stable oscillation. Obviously, if the inherent damping is zero, a neutrally stable oscillation already exists with zero dead spot.

Some additional calculations were made for the case where the airplane is disturbed within the dead spot. The motions for an initial condition of $\beta=1°$ were computed for $\eta=-2°$ and 0° with the assumption of the nonlinearity described in figure 1(b). The results are presented in figure 6. It should be noted that the only difference between figures 4 and 6 is the initial condition assumed in the calculations. In figure 6, the motion for $\eta=-2°$ is unstable and gradually approaches

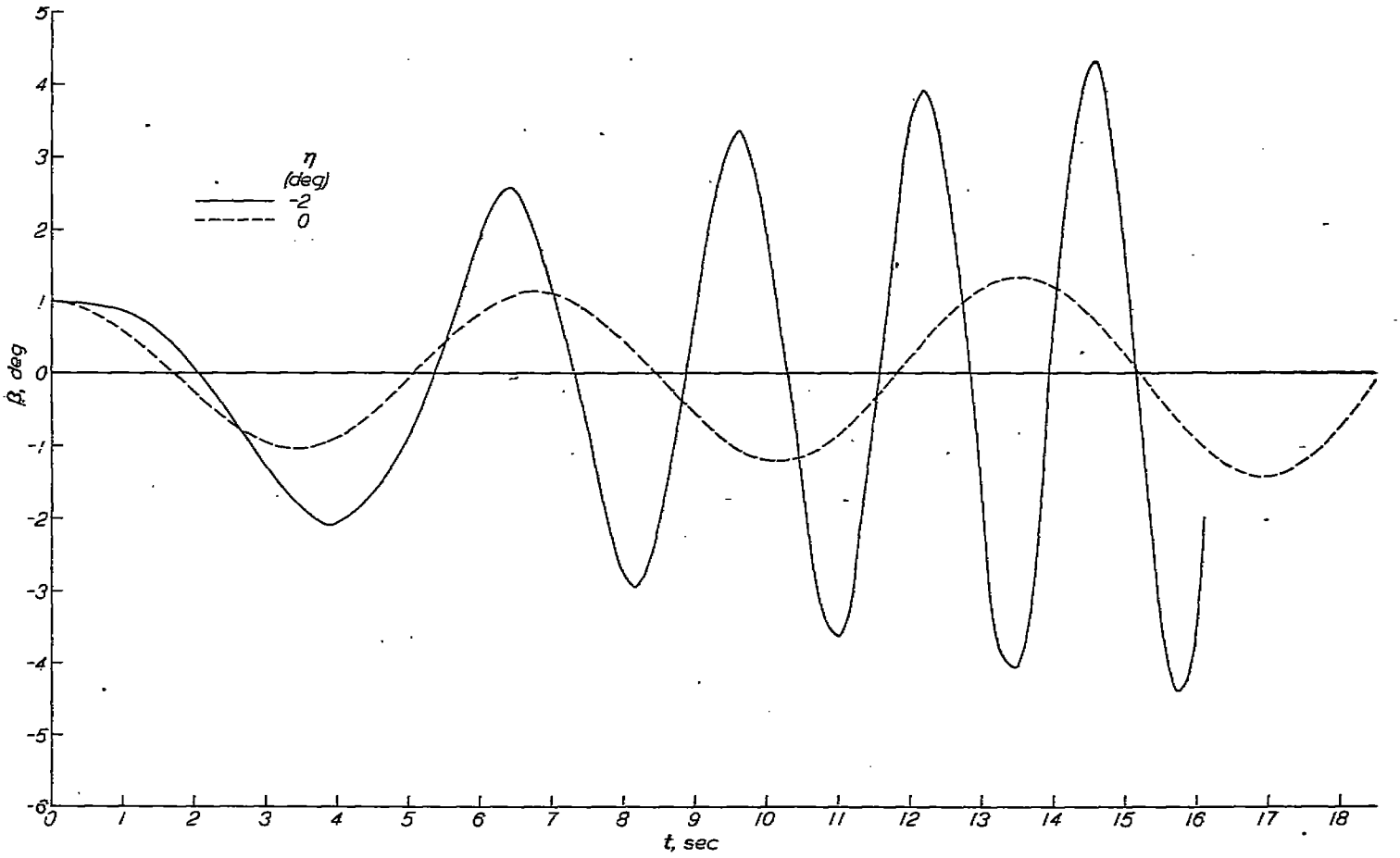

FIGURE 6.—The effect of the nonlinear derivatives described in figure 1(b) on the motion of an airplane. Initial disturbance in sideslip of 1°.

the amplitude and period of the motion for the case of $\eta=-2°$ in figure 4. The motion for $\eta=0°$ in figure 6 is slightly unstable and will probably increase until its amplitude and period are in close agreement with the motion for the case of $\eta=0°$ in figure 4. Calculations have indicated that the oscillatory motion of the airplane within the dead spot will double amplitude about every 4 seconds for $\eta=-2°$ and about every 30 seconds for $\eta=0°$. If the motion is unstable within the dead spot, either the airplane motion will be neutrally stable with an amplitude equal to or greater than the amplitude of the dead spot or the motion will be unstable.

The loss in damping and the increase in period which appeared in some of the lateral oscillations in figures 3 to 5 can be attributed to the type of nonlinearity assumed. From classical dynamic stability theory, it is well known that the damping of the oscillation is a function of C_{n_r} and the period of the oscillation is a function of C_{n_β}. If the airplane is considered as a mass-spring dashpot system, C_{n_β} is the equivalent spring constant of the system and C_{n_r} corresponds to the damping constant contributed by the dashpot. Thus as C_{n_β} is reduced the period increases, and as C_{n_r} is reduced the damping decreases.

213637—53——65

CONCLUDING REMARKS

The results of the investigation made to determine the effect of nonlinearities assumed in the analysis on the lateral stability indicate that under certain conditions a motion is obtained which has different rates of damping for the large and small amplitudes of motion, with very little damping at the small amplitudes. In general, the period of the resultant oscillation increases with time.

LANGLEY AERONAUTICAL LABORATORY,
NATIONAL ADVISORY COMMITTEE FOR AERONAUTICS,
LANGLEY FIELD, VA., *September 19, 1950.*

REFERENCES

1. Mokrzycki, G. A.: Application of the Laplace Transformation to the Solution of the Lateral and Longitudinal Stability Equations. NACA TN 2002, 1950.
2. Murray, Harry E., and Grant, Frederick C.: Method of Calculating the Lateral Motions of Aircraft Based on the Laplace Transform. NACA TN 2129, 1950.
3. Churchill, Ruel V.: Modern Operational Mathematics in Engineering. McGraw-Hill Book Co., Inc., 1944.